Fuzzy controller based Active Power Filter working in a Wind and PV Power Generation Systems using four leg inverter configurations.

A.SRINIVAS KUMAR
Godavari institute of engineering and technology
Affiliated to jntu kakinad ,india
Email id :srinivaskumar202@gmail.com

Abstract—An active power filter implemented with a four-leg voltage-source inverter using a predictive control scheme is presented. The use of a four-leg voltage-source inverter allows the compensation of current harmonic components, as well as unbalanced current generated by single-phase nonlinear loads. A detailed yet simple mathematical model of the active power filter, including the effect of the equivalent power system impedance, is derived and used to design the predictive control algorithm. This proposed system is placed in a wind and pv based power generation system. A Fuzzy logic controller is used in the control block to generate accurate control signals to the inverter circuit. The compensation performance of the proposed active power filter and the associated control scheme under steady state and transient operating conditions is demonstrated through simulations and experimental results.

Key words: wind and solar power plants, four leg inverter, active power filter, Satatic compensator, fuzzy logic controller.

INTRODUCTION

RENEWABLE generation affects power quality due to its nonlinearity, since solar generation plants and wind power generators must be connected to the grid through high-power static PWM converters [1]. The non uniform nature of power generation directly affects voltage regulation and creates voltage distortion in power systems. This new scenario in power distribution systems will require more sophisticated compensation techniques.

Although active power filters implemented with three-phase four-leg voltage-source inverters (4L-VSI) have already been presented in the technical literature [2]–[6], the primary contribution of this paper is a predictive control algorithm designed and implemented specifically for this application. Traditionally, active power filters have been controlled using pretuned controllers, such as PI-type or adaptive, for the current as well as for the dc-voltage loops [7], [8]. PI controllers must be designed based on the equivalent linear model, while predictive controllers use the nonlinear model, which is closer to real operating conditions. An accurate model obtained using predictive controllers improves the performance of the active power filter, especially during transient operating conditions, because it can quickly follow the current-reference signal while maintaining a constant dc-voltage.

So far, implementations of predictive control in power converters have been used mainly in induction motor drives [9]. In the case of motor drive applications, predictive control represents a very intuitive control scheme that handles multivariable characteristics, simplifies the treatment of dead-time compensations, and permits pulse-width modulator replacement. However, these kinds of applications present disadvantages related to oscillations and instability created from unknown load parameters . One advantage of the proposed algorithm is that it fits well in active power filter applications, since the power converter output parameters are well known . These output parameters are obtained from the converter output ripple filter and the power system equivalent impedance. The converter output ripple filter is part of the active power filter design and the power system impedance is obtained from well-known standard procedures. In the case of unknown system impedance parameters, an estimation method can be used to derive an accurate R–L equivalent impedance model of the system .This paper presents the mathematical model of the 4L-VSI and the principles of operation of the proposed predictive control scheme, including the design procedure. The complete description of the selected current reference generator implemented in the active power filter is also presented. Finally, the proposed active power filter and the effectiveness of the associated control scheme compensation are demonstrated through simulation and validated with experimental results obtained in a 2 kVA laboratory prototype.

FOUR-LEG CONVERTER MODEL

Fig. 1 shows the configuration of a typical power distribution system with renewable power generation. It consists of various types of power generation units and different types of loads. Renewable sources, such as wind and sunlight, are typically used to generate

electricity for residential users and small industries. Both types of power generation use ac/ac and dc/ac static PWM converters for voltage conversion and battery banks for long term energy storage. These converters perform maximum power point tracking to

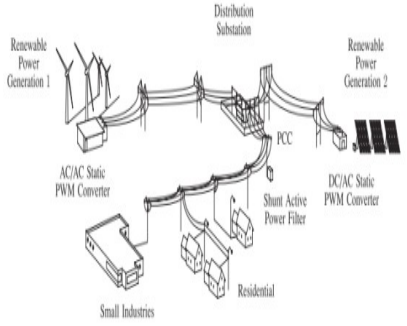

Fig. 1. Stand-alone hybrid power generation system with a shunt active power filter.

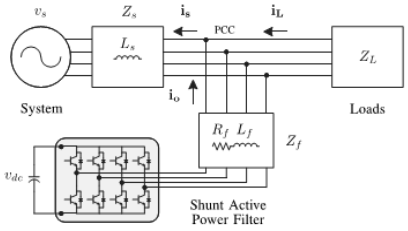

Fig. 2. Three-phase equivalent circuit of the proposed shunt active power filter

extract the maximum energy possible from wind and sun. The electrical energy consumption behavior is random and unpredictable, and therefore, it may be single- or three-phase, balanced or unbalanced, and linear or nonlinear. An active power filter is connected in parallel at the point of common coupling to compensate current harmonics, current unbalance, and reactive power. It is composed by an electrolytic capacitor, a four-leg PWM converter, and a first-order output ripple filter, as shown in Fig. 2. This circuit considers the power system equivalent impedance Zs, the converter output ripple filter impedance Z_f, and the load impedance Z_L.

The four-leg PWM converter topology is shown in Fig. 3. This converter topology is similar to the conventional three-phase converter with the fourth leg connected to the neutral bus of the system. The fourth leg increases switching states from 8 (23) to 16 (24), improving control flexibility and output voltage quality [21], and is suitable for current unbalanced compensation. The voltage in any leg x of the converter, measured from the neutral point (n), can be expressed in terms of switching states, as follows:

$$v_{xn} = S_x - S_n v_{dc}, x = u, v, w, n. \quad (1)$$

The mathematical model of the filter derived from the equivalent circuit shown in Fig. 2 is

$$V_0 = v_{xn} - R_{eq} i_0 - L_{eq} \frac{d i_0}{dt} \quad (2)$$

where *R*eq and *L*eq are the 4L-VSI output parameters expressed as Thevenin impedances at the converter output terminals *Z*eq .Therefore, the Thevenin equivalent impedance is determined by a series connection of the ripple filter impedance *Zf* and a parallel arrangement between the system equivalent impedance *Zs* and the load impedance *ZL*

$$Z_{eq} = \frac{Z_s Z_L}{Z_s + Z_L} + Z_f \approx Z_s + Z_f \quad (3)$$

For this model, it is assumed that $Z_L \_ Z_s$, that the resistive part of the system's equivalent impedance is neglected, and that the series reactance is in the range of 3–7% p.u., which is an acceptable approximation of the real system. Finally, in (2) $R_{eq} = R_f$ and $L_{eq} = Ls + L_f$.

DIGITAL PREDICTIVE CURRENT CONTROL

The block diagram of the proposed digital predictive current control scheme is shown in Fig. 4. This control scheme is basically an optimization algorithm and, therefore, it has to be implemented in a microprocessor. Consequently, the analysis has to be developed using discrete mathematics in order to consider additional restrictions such as time delays and approximations . The main characteristic of predictive control is the use of the system model to predict the future behavior of the variables to be controlled. The controller uses this information to select the optimum switching state that will be applied to the power converter, according to predefined optimization criteria. The predictive control algorithm is easy to implement and to understand, and it can be implemented with three main blocks, as shown in Fig. 4.

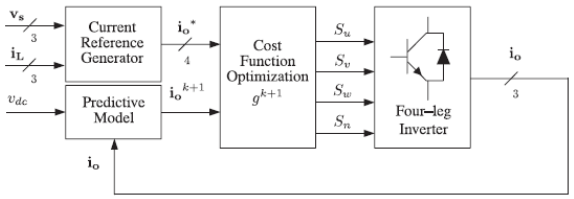

Fig. 4. Proposed predictive digital current control block diagram.

1) Current Reference Generator: This unit is designed to generate the required current reference that is used to compensate the undesirable load current components. In this case, the system voltages, the load currents, and the dc-voltage converter are measured, while the neutral output current and neutral load current are generated directly from these signals (IV).

2) Prediction Model: The converter model is used to predict the output converter current. Since the controller operates in discrete time, both the controller and the system model must be represented in a discrete time domain [22]. The discrete time model consists of a recursive matrix equation that represents this prediction system. This means that for a given sampling time T_s , knowing the converter switching states and control variables at instant kT_s , it is possible to predict the next states at any instant $[k + 1]Ts$ .Due to the first-order nature of the state equations that describe the model in (1)–(2), a sufficiently accurate first-order approximation of the derivative is considered in this paper.

$$\frac{dx}{dt} \approx \frac{x[k+1]-x[k]}{T s} \qquad (4)$$

The 16 possible output current predicted values can be obtained from (2) and (4) as

$$i_o[k+1]=\frac{T_s}{L_{eq}}\left(v_{xn}[k]-v_o[k]\right)+\left(1-\frac{R_{eq}T_s}{L_{eq}}\right)i_o[k] \quad (5$$

As shown in (5), in order to predict the output current i_o at the instant $(k + 1)$, the input voltage value v_o and the converter output voltage v_{xN} , are required. The algorithm calculates all 16 values associated with the possible combinations that the state variables can achieve.

3) Cost Function Optimization*:* In order to select the optimal switching state that must be applied to the power converter, the 16 predicted values obtained for **io**$[k + 1]$ are compared with the reference using a cost function g, as follows:

$$g[k+1]=\left(i^{*}_{ou}[k+1]-i_{ou}[k+1]\right)^2+\left(i^{*}_{ov}[k+1]-i_{ov}[k+1]\right)^2$$

$$+\left(i^{*}_{ow}[k+1]-i_{ow}[k+1]\right)^2+*$$

$$\left(i^{*}_{on}[k+1]-i_{on}[k+1]\right)^2 \qquad (6)$$

The output current (**io**) is equal to the reference (**i*o**) when $g = 0$. Therefore, the optimization goal of the cost function is to achieve a g value close to zero. The voltage vector $\mathbf{v_{xN}}$ that minimizes the cost function is chosen and then applied at the next sampling state. During each sampling state, the switching state that generates the minimum value of g is selected from the 16 possible function values. The algorithm selects the switching state that produces this minimal value and applies it to the converter during the $k + 1$ state.

CURRENT REFERENCE GENERATION

A dq-based current reference generator scheme is used to obtain the active power filter current reference signals. This scheme presents a fast and accurate signal tracking capability. This characteristic avoids voltage fluctuations that deteriorate the current reference signal affecting compensation performance [28]. The current reference signals are obtained from the corresponding load currents as shown in Fig. 5. This module calculates the reference signal currents required by the converter to compensate reactive power, current harmonic, and current imbalance. The displacement power factor $(\sin \varphi(L))$ and the maximum total harmonic distortion of the load $(\mathrm{THD}(L))$ defines the relationships between the apparent power required by the active power filter, with respect to the load, as shown

$$\frac{S_{APF}}{S_L}=\frac{\sqrt{\sin\varnothing_{(L)}+THD_{(L)^2}}}{\sqrt{1+THD_{(L)^2}}} \qquad (7)$$

where the value of $\mathrm{THD}(L)$ includes the maximum compensable harmonic current, defined as double the sampling frequency f_s . The frequency of the maximum current harmonic component that can be compensated is equal to one half of the converter switching frequency.

The dq-based scheme operates in a rotating reference frame; therefore, the measured currents must be multiplied by the $\sin(wt)$ and $\cos(wt)$ signals. By using dq-transformation, the d current component is synchronized with the corresponding phase-to-

neutral system voltage, and the *q* current component is phase-shifted by 90◦. The sin(*wt*) and cos(*wt*) synchronized reference signals are obtained from a synchronous reference frame (SRF) PLL [29]. The SRF-PLL generates a pure sinusoidal waveform even when the system voltage is severely distorted. Tracking errors are eliminated, since SRF-PLLs are designed to avoid phase voltage unbalancing, harmonics (i.e.,less than 5% and 3% in fifth and seventh, respectively), and offset caused by the nonlinear load conditions and measurement errors [30]. Equation (8) shows the relationship between the real currents $i_{Lx}(t)$ ($x = u, v,w$) and the associated *dq* components (*id* and *iq*)

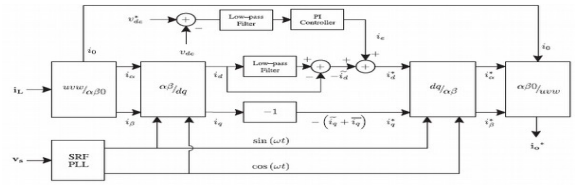

Fig. 5. *dq*-based current reference generator block diagram.

$$\begin{bmatrix} i_d \\ i_q \end{bmatrix} = \sqrt{\frac{2}{3}} \begin{bmatrix} \sin\omega t & \cos\omega t \\ -\cos\omega t & \sin\omega t \end{bmatrix} \begin{bmatrix} 1 & -\frac{1}{2} & -\frac{1}{2} \\ 0 & \frac{\sqrt{3}}{2} & -\frac{\sqrt{3}}{2} \end{bmatrix} \begin{bmatrix} i_{Lu} \\ i_{Lv} \\ i_{Lw} \end{bmatrix} \quad (8)$$

A low-pass filter (LFP) extracts the dc component of the phase currents i_d to generate the harmonic reference components $-\_i_d$. The reactive reference components of the phase-currents are obtained by phase-shifting the corresponding ac and dc components of i_q by 180◦. In order to keep the dc-voltage constant, the amplitude of the converter reference current must be modified by adding an active power reference signal i_e with the *d*-component, as will be explained in Section IV-A. The resulting signals i_d and i_q are transformed back to a three-phase system by applying the inverse Park and Clark transformation, as shown in (9). The cutoff frequency of the LPF used in this paper is 20 Hz

$$\begin{bmatrix} \dot{i}_{ou} \\ \dot{i}_{ov} \\ \dot{i}_{ow} \end{bmatrix} = \sqrt{\frac{2}{3}} \begin{bmatrix} \frac{1}{\sqrt{2}} & 1 & 0 \\ \frac{1}{\sqrt{2}} & \frac{-1}{2} & \frac{\sqrt{3}}{2} \\ \frac{1}{\sqrt{2}} & \frac{-1}{2} & \frac{-\sqrt{3}}{2} \end{bmatrix} \times \begin{bmatrix} 1 & 0 \\ 0 & \sin\omega t \\ 0 & \cos\omega t \end{bmatrix} \quad -cc \quad sir$$

The current that flows through the neutral of the load is compensated by injecting the same instantaneous value obtained from the phase-currents, phase-shifted by 180◦, as shown next

$$\dot{i}_{on} = -\left(i_{Lu} + i_{Lv} + i_{Lw}\right) \quad (10)$$

One of the major advantages of the *dq*-based current reference generator scheme is that it allows the implementation of a linear controller in the dc-voltage control loop. However, one important disadvantage of the *dq*-based current reference frame algorithm used to generate the current reference is that a second order harmonic component is generated in i_d and i_q under unbalanced operating conditions. The amplitude of this harmonic depends on the percent of unbalanced load current (expressed as the relationship between the negative sequence current i_L,2 and the positive sequence current i_L,1). The second-order harmonic cannot be removed from i_d and i_q , and therefore generates a third harmonic in the reference current when it is converted back to abc frame [31]. Fig. 6 shows the percent of system current imbalance and the percent of third harmonic system current, in function of the percent of load current imbalance. Since the load current does not have a third harmonic, the one generated by the active power filter flows to the power system.

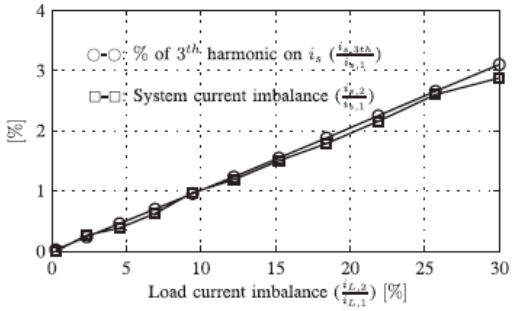

Fig. 6. Relationship between permissible unbalance load currents, the corresponding third-order harmonic content, and system current imbalance (with respect to positive sequence of the system current, *is*,1).

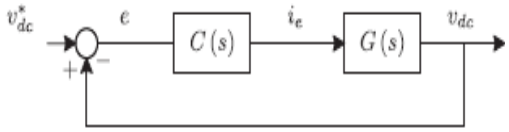

Fig. 7. DC-voltage control block diagram.

A. DC-Voltage Control

The dc-voltage converter is controlled with a traditional PI controller. This is an important issue in the evaluation, since the cost function (6) is designed using only current references, in order to avoid the use of weighting factors. Generally, these weighting factors are obtained experimentally, and they are not well defined when different operating conditions are required. Additionally, the slow dynamic response of the voltage across the electrolytic capacitor does not affect the current transient response. For this reason, the PI controller represents a simple and effective alternative for the dc-voltage control.

The dc-voltage remains constant (with a minimum value of 6 *vs*(rms)) until the active power absorbed by the converter decreases to a level where it is unable to compensate for its losses. The active power absorbed by the converter is controlled by adjusting the amplitude of the active power reference signal *ie* , which is in phase with each phase voltage. In the block diagram shown in Fig. 5, the dc-voltage *v*dc is measured and then compared with a constant reference value *v*∗ dc. The error (*e*) is processed by a PI controller, with two gains, K_p and T_i . Both gains are calculated according to the dynamic response requirement. Fig. 7 shows that the output of the PI controller is fed to the dc-voltage transfer function *Gs* , which is represented by a first-order system (11)

$$G(s)= \frac{v_{dc}}{i_c}=\frac{3}{2}\frac{K_p v_s\sqrt{2}}{C_{dc} v_{dc}^{¿}} \qquad (11)$$

The equivalent closed-loop transfer function of the given system
with a PI controller (12) is shown in (13)

$$C(s)= K_p\left(1+\frac{1}{T_i . s}\right) \qquad (12)$$

$$\frac{v_{dc}}{i_c}=\frac{\frac{\omega_n^2}{a}.(s+a)}{S^2+2\zeta\,\omega_n . s+\omega_n^2} \qquad (13)$$

Since the time response of the dc-voltage control loop does not need to be fast, a damping factor ζ = 1and a natural angular speed $\omega n = 2\pi \cdot 100$ rad/s are used to obtain a critically damped response with minimal voltage oscillation. The corresponding integral time $Ti = 1/a$ (13) and proportional gain *Kp* can be calculated as

$$\frac{3}{8}\frac{K_p v_s\sqrt{2}T_i}{C_{dc} v*¿_{dc}} \qquad (14)$$
$$\zeta=\sqrt{¿}$$

$$\omega_n .=\sqrt{\frac{3}{2}\frac{K_p v_s\sqrt{2}}{C_{dc} v_{dc}^{¿} T_i}} \qquad (15)$$

FUZZY LOGIC CONTROLLER

In FLC, basic control action is determined by a set of linguistic rules. These rules are determined by the system. Since the numerical variables are converted into linguistic variables, mathematical modeling of the system is not required in FC. The FLC comprises of three parts: fuzzification, interference engine and defuzzification. The FC is characterized as; i. seven fuzzy sets for each input and output. ii. Triangular membership functions for simplicity. iii. Fuzzification using continuous universe of discourse. iv. Implication using Mamdani‟s „min‟ operator. v. Defuzzification using the „height‟ method

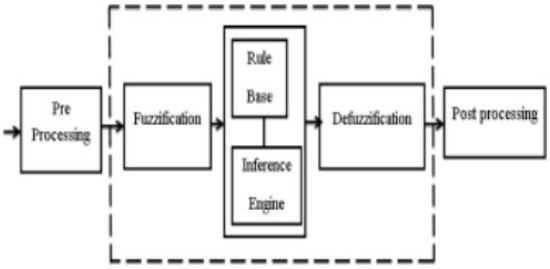

Fig.3 Fuzzy Logic Controller

Fuzzification:

Membership function values are assigned to the linguistic variables, using seven fuzzy subsets: NB (Negative Big), NM (Negative Medium), NS (Negative Small), ZE (Zero), PS (Positive Small), PM 5 (Positive Medium), and PB (Positive Big). The partition of fuzzy subsets and the shape of membership *CE(k) E(k)* function adapt the shape up to appropriate system. The value of input error and change in error are normalized by an input scaling factor

Change In Error	Error						
	NB	**N M**	**NS**	**Z**	**PS**	**PM**	**PB**
NB	PB	PB	PB	PM	PM	PS	Z
NM	PB	PB	PM	PM	PS	Z	Z
NS	PB	PM	PS	PS	Z	NM	NB
Z	PB	PM	PS	Z	NS	NM	NB
PS	PM	PS	Z	NS	NM	NB	NB
PM	PS	Z	NS	NM	NM	NB	NB
PB	Z	NS	NM	NM	NB	NB	NB

Table1. Fuzzy Rules

In this system the input scaling factor has been designed such that input values are between -1 and +1. The triangular shape of the membership function of this arrangement presumes that for any particular *E(k)* input there is only one dominant fuzzy subset. The input error for the FLC is given as

$$E(k) = \frac{P_{ph(k)} - P_{ph(k-1)}}{V_{ph(k)} - V_{ph(k-1)}}$$

$$CE(k) = E(k) - E(k-1)$$

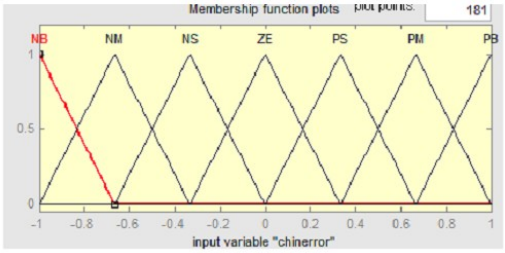

Membership Functions

Interference Method:

Several composition methods such as Max–Min and Max-Dot have been proposed in the literature. In this paper Min method is used. The output membership function of each rule is given by the minimum operator and maximum operator. Table 1 shows rule base of the FLC.

Defuzzification:

As a plant usually requires a non-fuzzy value of control, a defuzzification stage is needed. To compute the output of the FLC, „height" method is used and the FLC output modifies the control output. In recent years, the number and variety of applications of fuzzy logic have increased significantly. The applications range from consumer products such as cameras, camcorders, washing machines, and microwave ovens to industrial process control, medical instrumentation, decision-support systems, and portfolio selection. To understand why use of fuzzy logic has grown, you must first understand what is meant by fuzzy logic. Fuzzy logic has two different meanings. In a narrow sense, fuzzy logic is a logical system, which is an extension of multivalve logic. However, in a wider sense fuzzy logic (FL) is almost synonymous with the theory of fuzzy sets, a theory which relates to classes of objects with unsharp boundaries in which membership is a matter of degree. In this perspective, fuzzy logic in its narrow sense is a branch of fl. Even in its more narrow definition, fuzzy logic differs both in concept and substance from traditional multivalve logical systems.

In fuzzy Logic Toolbox software, fuzzy logic should be interpreted as FL, that is, fuzzy logic in its wide sense. The basic ideas underlying FL are explained very clearly and insightfully in Foundations of Fuzzy Logic. What might be added is that the basic concept underlying FL is that of a linguistic variable, that is, a variable whose values are words rather than numbers. In effect, much of FL may be viewed as a methodology for computing with words rather than numbers. Although words are inherently less precise than numbers, their use is closer to human intuition. Furthermore, computing with words exploits the tolerance for imprecision and thereby lowers the cost of solution.

Another basic concept in FL, which plays a central role in most of its applications, is that of a fuzzy if-then rule or, simply, fuzzy rule. Although rule-based systems have a long history of use in Artificial Intelligence (AI), what is missing in such systems is a mechanism for dealing with fuzzy consequents and fuzzy antecedents. In fuzzy logic, this mechanism is provided by the calculus of fuzzy rules. The calculus of fuzzy rules serves as a basis for what might be called the Fuzzy Dependency and Command Language (FDCL). Although FDCL is not used explicitly in the toolbox, it is effectively one of its principal constituents. In most of the applications of fuzzy logic, a fuzzy logic solution is, in reality, a translation of a human solution into FDCL. A trend that is growing in visibility relates to the use of fuzzy logic in combination with neuro computing and genetic algorithms. More generally, fuzzy logic, neuro computing, and genetic algorithms may be viewed as the principal constituents of what might be

called soft computing. Unlike the traditional, hard computing, soft computing accommodates the imprecision of the real world.

The guiding principle of soft computing is: Exploit the tolerance for imprecision, uncertainty, and partial truth to achieve tractability, robustness, and low solution cost. In the future, soft computing could play an increasingly important role in the conception and design of systems whose MIQ (Machine IQ) is much higher than that of systems designed by conventional methods Among various combinations of methodologies in soft computing, the one that has highest visibility at this juncture is that of fuzzy logic and neuro computing, leading to neuro-fuzzy systems. Within fuzzy logic, such systems play a particularly important role in the induction of rules from observations. An effective method developed by Dr. Roger Jang for this purpose is called ANFIS (Adaptive Neuro-Fuzzy Inference System). This method is an important component of the toolbox.

The fuzzy logic toolbox is highly impressive in all respects. It makes fuzzy logic an effective tool for the conception and design of intelligent systems. The fuzzy logic toolbox is easy to master and convenient to use. And last, but not least important, it provides a reader friendly and up-to-date introduction to methodology of fuzzy logic and its wide ranging applications.

SIMULATED RESULTS

A simulation model for the three-phase four-leg PWM converter with the parameters shown in Table I has been developed using MATLAB-Simulink. The objective is to verify the current harmonic compensation effectiveness of the proposed control scheme under different operating conditions. A six-pulse rectifier was used as a nonlinear load. The proposed predictive control algorithm was programmed using an S-function block that allows simulation of a discrete model that can be easily implemented in a real-time interface (RTI) on the dSPACE DS1103 R&D control board. Simulations were performed considering a 20 [μs] of sample time. In the simulated results shown in Fig. 8, the active filter startsto compensate at $t = t_1$. At this time, the active power filter injects an output current i_{ou} to compensate current harmonic components, current unbalanced, and neutral current simultaneously. During compensation, the system currents **is** show sinusoidal waveform, with low total harmonic distortion (THD = 3.93%).At $t = t_2$, a three-phase balanced load step change is generated from 0.6 to 1.0 p.u. The compensated system currents remain sinusoidal despite the change in the load current magnitude. Finally, at $t = t_3$, a single-phase load step change is introduced in phase u from 1.0 to 1.3 p.u., which is equivalent to an 11% current imbalance. As expected on the load side, a neutral current flows through the neutral conductor (i_{Ln}), but on the source side,no neutral current is observed (i_{sn}). Simulated results show that the proposed control scheme effectively eliminates unbalanced currents. Additionally, Fig. 8 shows that the dc-voltage remains stable throughout the whole active power filter operation.

TABLE I
SPECIFICATION PARAMETERS

VARIABLE	DESCRIPTION	VALUE
v_s	Source voltage	55[v]
f	System ferquency	50[Hz]
v_{dc}	dc-voltage	162[v]
C_{dc}	dc capacitor	2200[μF] (2.0pu)
L_f	Filter inductor	5.0[mH](0.5pu)
R_f	Internal resistance within L_f	0.6[Ω]
T_s	Sampling time	20[μs]
T_e	Execution time	16[μs]

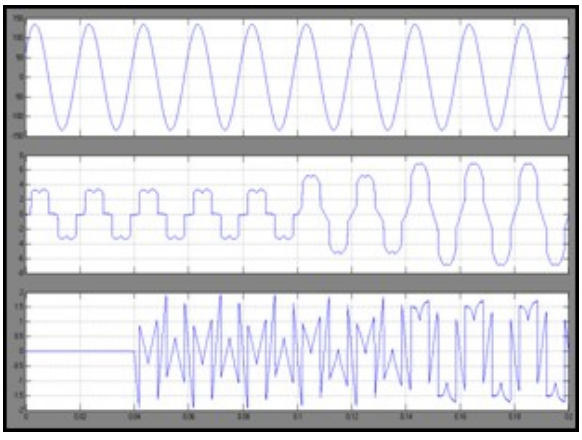

Fig. 8. Simulated waveforms of the proposed control scheme. (a) Phase to neutral source voltage. (b) Load Current. (c) Active power filter output current.

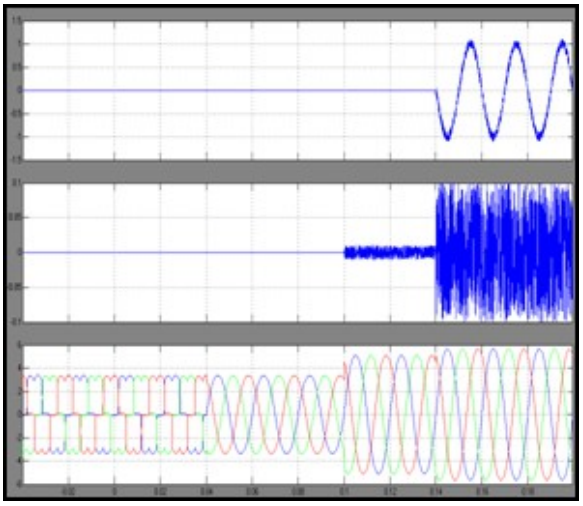

Fig. 8. Simulated waveforms of the proposed control scheme (d) Load neutral current. (e) System neutral current. (f) System currents

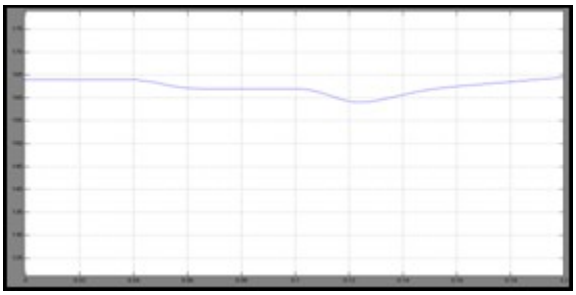

Fig. 8. Simulated waveforms of the proposed control scheme (g) DC voltage converter.

CONCLUSION

Improved dynamic current harmonics and a reactive power compensation scheme for power distribution systems with generation from renewable sources has been proposed to improve the current quality of the distribution system. Advantages of the proposed scheme are related to its simplicity, modeling, and implementation. The use of a predictive control algorithm for the converter current loop proved to be an effective solution for active power filter applications, improving current tracking capability, and transient response. Simulated and experimental results have proved that the proposed predictive control algorithm is a good alternative to classical linear control methods. The predictive current control algorithm is a stable and robust solution. Simulated and experimental results have shown the compensation effectiveness of the proposed active power filter.

REFERENCES

[1] J. Rocabert, A. Luna, F. Blaabjerg, and P. Rodriguez, "Control of power converters in AC microgrids," *IEEE Trans. Power Electron.*, vol. 27, no. 11, pp. 4734–4749, Nov. 2012.

[2] M. Aredes, J. Hafner, and K. Heumann, "Three-phase four-wire shunt active filter control strategies," IEEE Trans. Power Electron., vol. 12, no. 2, pp. 311–318, Mar. 1997.

[3] S. Naidu and D. Fernandes, "Dynamic voltage restorer based on a fourleg voltage source converter," Gener. Transm. Distrib., IET, vol. 3, no. 5, pp. 437–447, May 2009.

[4] N. Prabhakar and M. Mishra, "Dynamic hysteresis current control to minimize switching for three-phase four-leg VSI topology to compensate nonlinear load," IEEE Trans. Power Electron., vol. 25, no. 8, pp. 1935– 1942, Aug. 2010.

[5] V. Khadkikar, A. Chandra, and B. Singh, "Digital signal processor implementation and performance evaluation of split capacitor, four-leg and three h-bridge-based three-phase four-wire shunt active filters," Power Electron., IET, vol. 4, no. 4, pp. 463–470, Apr. 2011.

[6] F. Wang, J. Duarte, and M. Hendrix, "Grid-interfacing converter systems with enhanced voltage quality for microgrid application;concept and implementation," IEEE Trans. Power Electron., vol. 26, no. 12, pp. 3501– 3513, Dec. 2011.

[7] X.Wei, "Study on digital pi control of current loop in active power filter," in Proc. 2010 Int. Conf. Electr. Control Eng., Jun. 2010, pp. 4287–4290.

[8] R. de Araujo Ribeiro, C. de Azevedo, and R. de Sousa, "A robust adaptive control strategy of active power filters for power-factor correction, harmonic compensation, and balancing of nonlinear loads," IEEE Trans. Power Electron., vol. 27, no. 2, pp. 718–730, Feb. 2012.

[9] J. Rodriguez, J. Pontt, C. Silva, P. Correa, P. Lezana, P. Cortes, and U. Ammann, "Predictive current control of a voltage source inverter," IEEE Trans. Ind. Electron., vol. 54, no. 1, pp. 495–503, Feb. 2007.